



Integrated characterization of arabica coffee husk tea using flavoromics, targeted screening, and *in silico* approaches

Chunyan Zhao^b, Xiuwei Liu^a, Hao Tian^{a,*}, Zelin Li^{a,b,*}

^a Agro-Products Processing Research Institute, Yunnan Academy of Agricultural Sciences, Kunming 650223, China.

^b College of Food Science and Technology, Yunnan Agricultural University, Kunming 650201, China

ARTICLE INFO

Chemical compounds studied in this article:

Hexanal (PubChem CID: 6184)
 Octanal (PubChem CID: 454)
 Furfural (PubChem CID: 7362)
 2-Heptanol (PubChem CID: 10976)
 2,3-Butanediol (PubChem CID: 262)
 Benzyl alcohol (PubChem CID: 244)
 6-Methyl-5-hepten-2-one (PubChem CID: 9862)
 Butyrolactone (PubChem CID: 7302)
 Damascenone (PubChem CID: 5366074)
 1-Methylnaphthalene (PubChem CID: 7002)

Keywords:

Coffee husk tea
 Volatile compounds
 Olfactory characteristics
 Antioxidant
 Anti-inflammation
 Molecular simulation

ABSTRACT

This study aimed to identify the key volatile compounds in two types of processed arabica coffee husk tea, elucidate their olfactory characteristics, and investigate their antioxidant and anti-inflammatory activities. Sensory evaluation indicated differences between the two groups. A total of 64 and 99 compounds were identified in the C and FC groups, respectively, with 5 identified as key aroma compounds (ROAV \geq 1). Molecular simulations indicated that four common key aroma compounds were successfully docked with OR1A1 and OR5M3 receptors, forming stable complexes. Furthermore, 14 volatile compounds interacted with 140 targets associated with oxidation and inflammation, linking to 919 gene ontology (GO) terms and 135 kyoto encyclopedia of genes and genomes (KEGG) pathways. Molecular simulations revealed that these volatile components showed antioxidant and anti-inflammatory effects by interacting with core receptors through several forces, including van der Waals, Pi-alkyl, and Pi-cation interactions and hydrogen bonds.

1. Introduction

Coffee husks represent the initial by-product generated during coffee production, comprising approximately 45–50% of the coffee cherries and an yielding around 160,000 tons annually (Li, Wei, et al., 2023; Li, Wu, et al., 2023; Li, Yuan, et al., 2023; Li, Zhou, et al., 2023). The rational utilization of coffee husks has emerged as a global imperative demanding resolution. However, improper handling of coffee husks can result in rapid structural degradation and environmental contamination, posing a risk to human health (Fernandes et al., 2017). Using coffee husks as a food source, such as in coffee husk tea preparation, is a rational approach due to their abundant bioactive compounds, which offer significant health benefits (Sales, Cunha, et al., 2023; Sales, Iriundo-DeHond, et al., 2023). Coffee husk tea is referred to by a variety of names in different countries, including “sultana” in Bolivia, “qishr” in Yemen, “hashara” in Ethiopia, and “cascara” in El Salvador and

Colombia (DePaula et al., 2022). Traditionally, it has been consumed as a tea-like beverage or medicinal infusion, appreciated for its delectable taste profile and nutritional attributes (DePaula et al., 2022). The production of coffee husk tea involves using husks from fully matured coffee cherries, which undergo various drying techniques. The European Food Safety Authority (EFSA) authorized the application of coffee husk tea as a novel food in the European market (Sales, Cunha, et al., 2023; Sales, Iriundo-DeHond, et al., 2023). Considering the intrinsic coffee husk tea and its historical consumption as a food, EFSA has deemed further toxicological investigations unnecessary while asserting a minimal risk of allergic reactions (Sales, Cunha, et al., 2023; Sales, Iriundo-DeHond, et al., 2023). Nevertheless, coffee is susceptible to mycotoxin contamination, especially ochratoxins which are classified as possibly carcinogenic to humans (Group 2B) by the International Agency for Research on Cancer (IARC) (Paterson et al., 2014). Hence, the correct utilization of the coffee husk holds significant importance.

* Corresponding authors at: Agro-Products Processing Research Institute, Yunnan Academy of Agricultural Sciences, Kunming 650221, China.

E-mail addresses: tianhao@yaas.org.cn (H. Tian), lzl1054994094@126.com (Z. Li).

<https://doi.org/10.1016/j.fochx.2024.101556>

Received 4 March 2024; Received in revised form 9 June 2024; Accepted 12 June 2024

Available online 18 June 2024

2590-1575/© 2024 The Author(s). Published by Elsevier Ltd. This is an open access article under the CC BY-NC-ND license (<http://creativecommons.org/licenses/by-nc-nd/4.0/>).

In China, coffee husks have traditionally been used to prepare tea-like beverages over an extended period of time. The coffee husk tea has been reported to exhibit potent *in vitro* antioxidant, anti-inflammatory, antibacterial, adipogenic, and lipolytic properties (Heeger et al., 2017; Sales, Cunha, et al., 2023; Sales, Iriando-DeHond, et al., 2023). The aroma of infused coffee husk tea has aromatically sweet, floral, tea-like, herbal, woody, prune-like, fruity, and honey notes (DePaula et al., 2022; Kristanti et al., 2022). A previous study demonstrated that the aromas could exhibit their olfactory characteristics by binding the OR8D1, OR7D4, OR5M3, OR2W1, OR1G1, and OR1A1 receptors to form van der Waals, Pi-sigma, Pi-alkyl, alkyl, and Pi-cation interactions and hydrogen bonds after the molecular docking analysis (Mei et al., 2023). To date, there is still a lack of literature on the identification and characterization of key aroma compounds in coffee husk tea, along with their corresponding biological activities.

Certain aroma compounds derived from plants exhibit distinct aromatic characteristics and significant biological activities. Monoterpenes are associated not only with fruity, floral, and minty aromas but also exhibit several bioactivities, including antimicrobial, antidiabetic, hepatoprotective, cardioprotective, and neuroprotective effects (Paulino et al., 2022). The aroma compound β -ionone is found in various plant organs, including roots, stems, leaves, flowers, and fruits. It possesses several beneficial effects on human health, such as anti-cancer, antibacterial, anti-inflammatory, antimicrobial activities and regulation of blood lipid levels (Hou et al., 2023; Huang et al., 2024). Volatile compounds such as N-capric acid isopropyl ester, (*E*)-octadec-11-enoic acid, and 2H-pyran-2,4(3H)-dione found in *Synechococcus* sp. biomass have been identified as potential regulators for Alzheimer's disease (Xie, Chen, et al., 2023; Xie, Wang, et al., 2023). Network pharmacology offers a means to investigate the intricate interplay among drugs, components, targets, and diseases, providing a highly efficient approach for the targeted screening of potent molecules within complex mixtures (Mei & Chen, 2023). Furthermore, the computer-based techniques such as molecular docking and molecular dynamics simulation analysis are effective methods for evaluating the binding affinity and stability of the complex (Zhao et al., 2024).

In this study, the volatile compounds from two different arabica coffee husk tea processing methods were identified, and their odor characteristics, along with potential antioxidant and anti-inflammatory activities, were investigated using flavoromics, targeted screening, and *in silico* methodologies.

2. Materials and methods

2.1. Coffee husk tea samples

Fresh arabica coffee cherries were harvested from Baoshan City, Yunnan Province, China. Subsequently, the coffee husks, free from any pests, diseases, or signs of decay, were used to produce husk tea and comprised two groups (Fig. S1). In the coffee husk tea (C) group, 5 kg fully mature coffee cherries were washed, drained, peeled, and dried at 45 °C to approximately 5% moisture content. In the fermented coffee husk tea (FC) group, the samples were treated the same way as the C group, followed by fermentation of the husks in the fermenter (23 ± 1 °C) to induce anaerobic conditions, according to the method described by Batista Da Mota et al.'s (2022) methods with some modifications. Each fermenter was filled with approximately 10 L of pulped coffee husks for 48 h fermentation (Fig. S1). Subsequently, all samples were dried to achieve a moisture content of 5%. A total 20 g was randomly weighed six times from a 1 kg sample as six biological replicates ($n = 6$).

2.2. Chemicals

The 2-methyl-3-heptanone (purity >99%) was purchased from Sigma-Aldrich Corporation (MO, USA). Helium (He, purity >99.999%) was purchased from Wuhan Newride Trading Co., Ltd. (Wuhan, China).

The DB-WAX (30 m × 0.25 mm × 0.25 μ m) column was purchased from Agilent Technologies(CA, USA).

2.3. Sensory evaluation

The samples (20 g) were placed in a beaker, and 100 mL of boiling water was added for rapid brewing. The water was promptly decanted, and the samples were incubated for 30 s. Subsequently, another 100 mL of boiling water was added, and sensory evaluation was conducted once the temperature was below 50 °C.

Professional panelists comprising four males and five females with an average age of 30 years, were recruited from Yunnan Agricultural University in China. The panelists had been trained to evaluate the sensory characteristic of tea and different beverages according to the Chinese national standard procedure (Li, Wei, et al., 2023; Li, Wu, et al., 2023; Li, Yuan, et al., 2023; Li, Zhou, et al., 2023). After the training, a comprehensive discussion was conducted to precisely determine the appropriate terminology for describing the flavor characteristics of both coffee husk teas. Before the commencement of the sensory experiment, all participants were thoroughly briefed on the experimental details, and their informed consent was obtained. The study protocol received ethical approval from the Research Ethics Committee of Yunnan Agricultural University. The sensory attributes assessed included aromatic, acidity, fatty, medicine-like, grassy, floral, fruity, sweet, and after-taste characteristics. The maximum score for each sensory attributes was 5. Each panelist rated the quality of the two coffee husk tea samples by a multi-index comprehensive evaluation method.

2.4. Analysis of volatile compounds

2.4.1. HS-SPME extraction

The headspace solid-phase microextraction (HS-SPME) was used for volatile compound extraction according to the method of Li, Wei, et al. (2023), Li, Wu, et al. (2023), Li, Yuan, et al. (2023) and Li, Zhou, et al. (2023) with some modifications. Briefly, the 50/30 μ m divinylbenzene/carboxen/polydimethylsiloxane (DVB/CAR/PDMS) extraction head (Supelco, Bellefonte, USA) was first heated at 250 °C for 15 min to eliminate the effects of impurities. Chopped finger citron samples (2 g) was weighed into a 20 mL headspace bottle and brewed with 10 mL boiling water following the Section 2.3. Afterward, 5 mL of the sample was supplemented with a 10 μ L aliquot of an internal standard solution containing 2-methyl-3-heptanone (0.408 mg/mL) for testing.

2.4.2. GC-MS analysis

An Agilent 7890B–5977B gas chromatography–mass spectrometry (GC-MS) system (Agilent Technologies, CA, USA) equipped with a DB-WAX (30 m × 0.25 mm × 0.25 μ m) column was used for volatile compound detection according to the method of Xu et al. (2022) with some modifications. He was used as carrier gas with a flow rate of 1 mL/min. The injector temperature was maintained at 260 °C with a splitless inlet. The temperature in the GC oven was maintained at 40 °C for 5 min, and then raised to 220 °C at a rate of 5 °C/min and to 250 °C at a rate of 20 °C/min and maintained for 2.5 min. MS condition setup was as follows: electron ionization source was used with an electron energy of 70 eV, a ion source temperature 230 °C, a quadrupole temperature 150 °C and a full scan mode (20–400 m/z).

2.4.3. Qualitative and quantitative of volatile compounds

The recorded mass spectra was compared with the National Institute of Standards and Technology (NIST) 14.0 database to qualitative and quantitative the volatile compounds. The retention index (RI) was calculated by using the retention time of n-alkanes as the standard and combined with the known RI for the characterization (Xu et al., 2022). The retention index was calculated as shown in Eq. (1).

$$RI = 100 \times n + \frac{100(T_V - T_n)}{T_{n+1} - T_n} \quad (1)$$

T_V , retention time of chromatographic peak of volatile compounds; T_n , T_{n+1} , retention time of n-alkanes C_n and C_{n+1} .

The relative content of each volatile compound was calculated based on the peak area normalization method (Eq. 2).

$$\text{Relative content (\%)} = \frac{M}{N} \times 100\% \quad (2)$$

M , peak area of aroma compounds of individual component. N , overall peak area.

2.4.4. Determination of relative olfactory activity value (ROAV)

The ROAV_{*i*} of the component that contributes the most to the overall flavor of the sample was defined as 100, the ROAV of other components (*i*) was calculated according to the Eq. (3) (Li, Wei, et al., 2023; Li, Wu, et al., 2023; Li, Yuan, et al., 2023; Li, Zhou, et al., 2023).

$$ROAV_i \approx \frac{C_i \times T_{\max}}{C_{\max} \times T_i} \times 100 \quad (3)$$

C_i , the content of an aroma compound in sample (%), T_i , the aroma threshold of a compound in water ($\mu\text{g}/\text{kg}$); C_{\max} and T_{\max} , the relative content and aroma threshold of the compound that contributed the most to the sample flavor, respectively.

2.5. Target prediction

To explore the potential antioxidant and anti-inflammatory effects of 14 key aroma compounds identified from Section 2.4, the targeted network screening was conducted. The SMILES number of 14 key aroma compounds was obtained from the PubChem database (<https://pubchem.ncbi.nlm.nih.gov/>). The compounds targets were collected using the Swiss Target Prediction database (<http://www.swisstargetprediction.ch/>) and TargetNet database (<http://targetnet.scbdd.com/calcnet/index/>).

The oxidative stress and inflammation related targets were collected through DisGeNet database (<http://www.disgenet.org/>, with a score of ≥ 0.3), and GeneCards database (<https://www.genecards.org/>, with a relevance score of ≥ 2) (Hong et al., 2023; Mei & Chen, 2023). These targets were combined and duplicates were removed and considered as relevant targets for oxidative stress and inflammation. Venn diagrams of compounds and the oxidative stress and inflammatory targets were drawn using the Bioinformatics website (<https://www.bioinformatics.com.cn/>).

2.6. Network and pathway construction

A network connecting the targets of key volatile compounds in arabica coffee husk tea with oxidative stress and inflammation-related targets was established based on a previous study (Cai et al., 2023). Briefly, the Network Analyzer (Cytoscape 3.8.2 software, University of California, San Diego, California, USA) and the STRING 12.0 database (<https://string-db.org/>) were used to generate a protein-protein interaction (PPI) network with a minimum required interaction score of 0.7. The network topology parameters (degree) and key targets were then determined. Furthermore, GO and KEGG pathway enrichment analyses were performed using the DAVID database (<https://DAVID.ncifcrf.gov/>), with the top 10 pathways determined based on their *p*-values.

2.7. Molecular docking analysis

Molecular docking analysis was performed following the method described by Mei et al. (2023). The information on ligands and receptors is presented in Table S1. The center coordinates were set as $x = 47.25 \text{ \AA}$,

$y = 34.50 \text{ \AA}$, $z = 47.25 \text{ \AA}$. Docking and visual analysis of the three-dimensional (3D) and two-dimensional (2D) binding processes were performed using PyMOL (DeLano Scientific LLC, USA), AutoDockTool 1.5.7 (Scripps Research, USA), and Discovery Studio 2019 (BIOVIA Inc., France) software.

2.8. Molecular dynamic simulations

Molecular dynamic simulations of complexes OR1A1–2-heptanol, OR1A1–butyrolactone, OR5M3–damascenone, HSP90AA1–benzyl alcohol, TNF–benzyl alcohol, and SRC–benzyl alcohol were performed using AMBER 18 software. The preparation for molecular dynamics simulation followed the methodology outlined by Salomon-Ferrer et al. (2013). Subsequently, molecular dynamic simulations were conducted for 100 ns. The root-mean-square deviation (RMSD), radius of gyration (RoG), solvent accessible surface area (SASA), and number of hydrogen bonds were computed to assess the stability of the seven complex systems.

2.9. Statistical analysis

All experiments were conducted six times. Spider diagrams and principal component analysis (PCA) were generated using Origin 2022 software (OriginLab Co., LTD, USA). Multivariate analysis, including heat map and partial least squares discriminant analysis (PLS-DA), were performed using SIMCA-P 14.1 software (Umetrics Co., LTD, Sweden). One-way analysis of variance followed by Duncan's *post hoc* analysis was performed using SPSS Statistics version 21 software (IBM, NY, USA). $p < 0.05$ was considered statistically significant difference.

3. Results and discussion

3.1. Sensory evaluation of coffee husk tea

The spider diagram in Fig. 1a illustrates the sensory scores of the two sample groups. Differences in sensory attributes were observed between the C and FC groups. Specifically, the FC group showed decreased aromatic, acidity, after-taste, and grassy flavors while showing increased intensity in sweet and medicine-like qualities compared to the C group. These observations could be associated with the metabolic activity of microorganisms during fermentation, resulting in the consumption of nutrients such as sugars and proteins, thereby decreasing the formation of flavor compounds. Additionally, fermentation induced changes in the composition of flavor precursors, consequently contributing to differences in aroma profiles during the brewing process (Sales, Cunha, et al., 2023; Sales, Iriondo-DeHond, et al., 2023).

3.2. Volatile compounds identification and screening

A total of 10,110 peaks were detected in the total ion chromatograms of both groups of coffee husk tea (Fig. S2). Further screening identified 64 and 99 volatile compounds with chemical abstracts service (CAS) numbers in the C and FC groups, respectively (Supplementary Data). PCA and PLS-DA revealed complete separation of the samples into two clusters, with further permutation tests confirming no over fitting (Fig. 1b-c). These results indicated that different processing methods for coffee husk tea could lead to different flavor profiles. Furthermore, compounds with variable importance for the projection (VIP) scores > 1 and *p*-value < 0.05 were considered significantly different. A total of 14 volatile compounds, including 3 aldehydes, 3 alcohols, 3 ketones, 2 naphthalenes, and 3 others, were identified as significantly different (Fig. 1d and Table 1). Additionally, 5 key volatile compounds (ROAV ≥ 1) were identified (Table 1). Consequently, the C group exhibited higher abundances of "acidity", "floral", "green", and "fatty" aromas, while the FC group showed a greater prevalence of "medicine-like" and "sweet" aromas. These findings were subjected to further

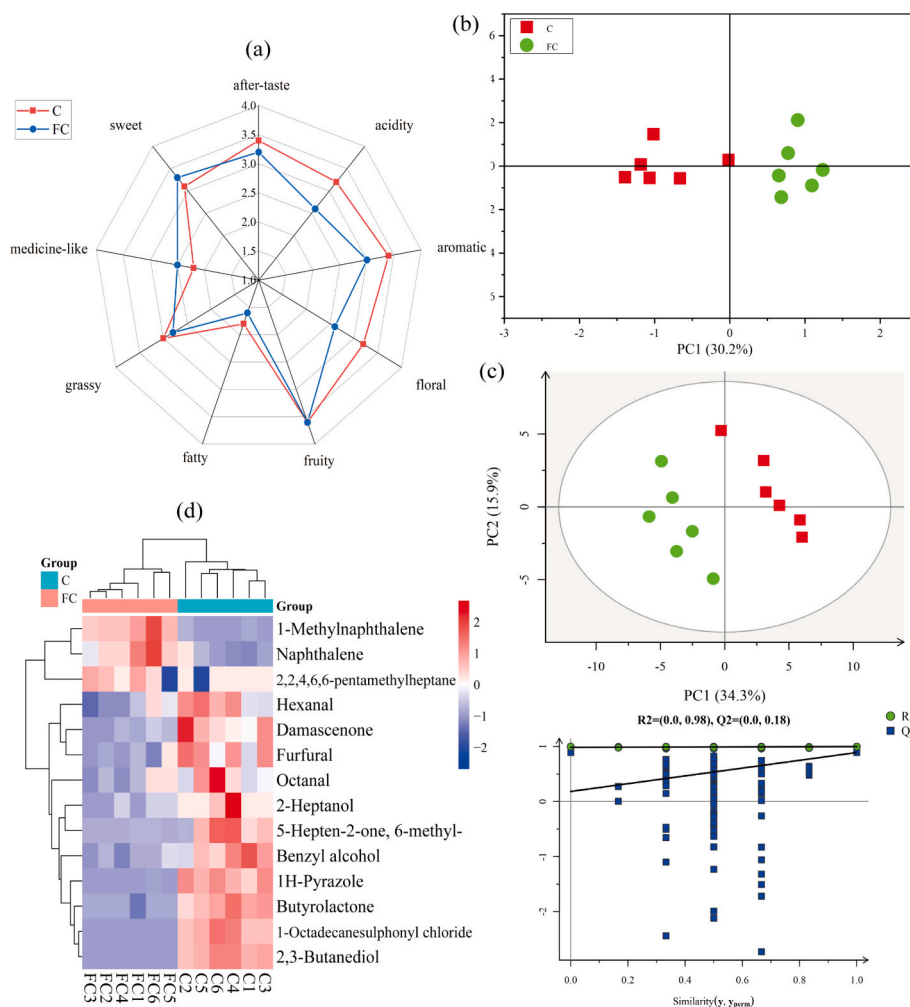


Fig. 1. Sensory evaluation and multivariate statistical analysis. (a) Sensory evaluation of C and FC group samples; (b) principal component analysis (PCA); (c) partial least square discriminate analysis (PLS-DA) and its permutation test; (d) heatmap of different volatile compounds.

discussion.

The ROAV is commonly used to assess the contribution of volatile compounds to aroma. A ROAV value greater than one generally indicates a crucial contribution of the volatile compound to the aroma, while between 0.1 and 1 suggest that the compound has some effects on the aroma (Li, Wei, et al., 2023; Li, Wu, et al., 2023; Li, Yuan, et al., 2023; Li, Zhou, et al., 2023). It has been demonstrated that volatile aldehydes and alcohols are essential components contributing to coffee aroma (Wang et al., 2023). Aldehydes are characteristic flavor substances with low thresholds (Lin et al., 2024). Hexanal, an oxidation product of linoleic acid contributes to fresh, green, fatty, and grassy aromas (Xie, Chen, et al., 2023; Xie, Wang, et al., 2023). Furfural can produce a roasted coffee bean-like, fragrant, bread, woody, sweet, caramel, and cinnamon odors (Gao et al., 2023; Wang et al., 2023). Octanal has significant fatty, fruity, orange peel, and lemon aroma characteristics (Fang et al., 2024). Among these three aldehydes, only hexanal in the C group demonstrated an ROAV >1, indicating a higher contribution to grassy and green odors within this subgroup (Table 1). Conversely, all ROAV values for different volatile aldehydes in the FC group were lower than those in the C group, suggesting that self-induced anaerobic fermentation had a modifying effect (Table 1).

Alcohols typically contribute distinct floral, sweet, and fruity aromas, which harmonize effectively with beverage aromas (Li, Wei, et al., 2023; Li, Wu, et al., 2023; Li, Yuan, et al., 2023; Li, Zhou, et al., 2023). They also serve as an aromatic compound in coffee husk. 3-Heptanol was detected in wet primary processing treatments of arabica

coffee husk with arctic bramble, melon, fruit-fresh, and mushroom aromas (Li, Wei, et al., 2023; Li, Wu, et al., 2023; Li, Yuan, et al., 2023; Li, Zhou, et al., 2023; Wan et al., 2024). In this study, 2-heptanol was detected in both sample groups with ROAV values >1 (Table 1), and the FC group showed lower levels than the C group. This observation could be attributed to fermentation depleting the contents of coffee husk.

Ketones are commonly associated with tallow, burnt, and floral aromas, which gradually intensify with the elongation of the carbon chain (Xu et al., 2024). Butyrolactone and damascenone, with remarkably low odor thresholds, significantly contribute to the “floral” and “fruit” aroma profiles (Lan et al., 2021; Tian et al., 2023). Butyrolactone and damascenone had ROAV values of >10 in both sample groups (Table 1), indicating the significant influence of ketones on the aromatic profile of coffee husk tea. Ketones primarily originate from processes such as the Maillard reaction, thermal modification of amino acids in food, and oxidation of free fatty acids (Sevindik et al., 2022). Therefore, differences in aroma between the two groups may have emerged during the brewing process. Naphthalene belongs to a class of polycyclic aromatic hydrocarbon compounds known for their distinctive pungent naphthyl and sweet odors (Li et al., 2024). This is consistent with the evaluation findings. Aroma contribution analysis through network analysis revealed a complex correlation among the aromas of differential volatile compounds (Fig. S3), suggesting that the presence of one aroma compound could either enhance or suppress the perception of another. Therefore, this interplay is also one of the factors contributing to the variations in aroma observed among different types of tea made

Table 1
Aroma characteristics and ROAV values of 14 key different volatile compounds.

No.	Volatile compounds	RT (min)	RI		OT (µg/kg)	Odor description	Relative content (%)		ROAV	
			Calculate	Reference			C	FC	C	FC
1	Hexanal	7.86	1102	1090	4.50 ^a	Fresh, green, fatty, grassy	5.34 ± 0.95	3.62 ± 0.86	1.59	1.08
2	Octanal	14.32	1311	1301	3.4 ^b	Fatty, fruity, orange peel, lemon	1.43 ± 0.41	1.04 ± 0.25	0.57	0.41
3	Furfural	19.20	1439	1462	282 ^c	Fragrant, bread, woody, sweet, caramel, cinnamon, baked, almond	4.06 ± 0.83	2.41 ± 0.57	0.02	0.01
4	2-Heptanol	15.64	1346	1318	0.1 ^h	Arctic bramble, melon, fruit-fresh, mushroom, lemon, citrus	1.97 ± 0.94	0.69 ± 0.27	26.48	9.2
5	2,3-Butanediol	22.33	1520	1553	95.1 ⁱ	Fruity, onion	3.52 ± 0.51	0.03 ± 0.00	0.05	0.00
6	Benzyl alcohol	28.89	1690	1821	100 ^a	Aromatic, floral, sweet, bitter almond	1.32 ± 0.26	0.75 ± 0.11	0.02	0.01
7	6-Methyl-5-hepten-2-one	15.83	1351	1337	50 ^{ac}	Pepper, apple, mushroom, citrus, musty, rubber, nutty, green, hazelnut, bitter, lemongrass	0.46 ± 0.26	0.03 ± 0.00	0.12	0.00
8	Butyrolactone	23.30	1546	1595	0.02 ^e	Apple, pineapple, sweet, caramel	1.13 ± 0.19	0.24 ± 0.10	75.94	16.13
9	Damascenone	27.77	1762	1774	0.05 ^f	Roses, plums, pomelo, raspberries, apple, honey, tobacco, sweet	3.72 ± 1.23	1.48 ± 0.29	100	39.78
10	1-Methylnaphthalene	28.26	1774	1844	0.1 ^g	medicinal, sweet, vanilla-like	0.18 ± 0.06	1.31 ± 0.33	2.42	17.61
11	Naphthalene	25.81	1611	1694	6.00 ^d	Phenolic, mothballs, greasy, oily, pungent, tarry	0.51 ± 0.14	0.92 ± 0.21	0.11	0.21
12	1H-Pyrazole, 4,5-dihydro-5,5-dimethyl-4-isopropylidene-	22.60	1527	–	–	–	0.82 ± 0.14	0.03 ± 0.00	–	–
13	2,2,4,6,6-Pentamethylheptane	4.47	855	915	–	Alkane-like	0.83 ± 0.39	0.97 ± 0.48	–	–
14	1-Octadecanesulphonyl chloride	17.57	1398	–	–	Wax-like	1.40 ± 0.27	0.03 ± 0.00	–	–

Note: “–”: not detected. a: (Xie, Chen, et al., 2023; Xie, Wang, et al., 2023); b: (Fang et al., 2024); c: (Gao et al., 2023); d: (Li et al., 2024); e: (Tian et al., 2023); f: (Lan et al., 2021); g: (Liang et al., 2022); h: (Li, Wei, et al., 2023; Li, Wu, et al., 2023; Li, Yuan, et al., 2023; Li, Zhou, et al., 2023); i: (Giri, Osako, & Ohshima, 2010).

from coffee husk.

3.3. Simulation analysis of key aroma perception

Elucidating the binding characteristics and differential mechanisms between ligands and receptors through molecular docking is crucial for understanding fundamental biological processes (Harini & Sowdhamini, 2015). Four key differential compounds (ROAV > 1) in the two coffee husk tea samples, namely, 2-heptanol, butyrolactone, damascenone, and 1-methylnaphthalene, predominantly contributed the aroma profiles of “floral”, “fruity”, “fatty”, “sweet”, and “medicine-like”. However, some 1-methylnaphthalene might be produced in the SPME extraction process. Therefore, 2-heptanol, butyrolactone, damascenone were used to investigate their binding interactions with six of the most widely studied olfactory receptors, including OR8D1, OR7D4, OR5M3, OR2W1, OR1G1, and OR1A1 (Mei et al., 2023). The binding affinity of the above three compounds to these six olfactory receptors, as presented in Table S2, was lower than -3.1 kcal/mol, indicating a spontaneous interaction between them. Butyrolactone and 2-heptanol showed the most favorable binding energies (-4.5 and -5.0 kcal/mol, respectively) with the OR1A1 receptor. Notably, the complexes formed between OR1A1 and 2-heptanol or butyrolactone were engaged in four hydrogen bonds at Asn109, Ile105, Asn109, and Asn155 residues (Fig. 2a-b). Moreover, these compounds showed hydrophobic interactions with Phe206, Val203, Tyr258, Val254, Phe206, Gly202, Asn155, and Try258 at the binding site of OR1A1 (Table S2). These results suggested that butyrolactone and 2-heptanol of arabica coffee husk tea might generate fruity, fresh, and sweet aromas by activating OR1A1. The damascenone compounds exhibited the highest binding affinity (-7.6 kcal/mol) towards OR5M3, forming six hydrophobic interactions at Ala201, Phe205, Tyr250, Leu253, Ile254, and Try257 (Table S2 and Fig. 2c). Previous research has shown that hydrophobic amino acid residues create a favorable hydrophobic environment for odorants, facilitating their

stable binding (Sun et al., 2024). These results implied that activation of the OR5M3 receptor may potentially generate “floral” aromas.

In this study, the stability and binding ability of the four complexes, including OR1A1–2-heptanol, OR1A1–butyrolactone, and OR5M3–damascenone were further investigated using molecular dynamic simulation. RMSD serves as a quantitative indicator of the system's stability. The fluctuation of RMSD values of the complexes remained within a reasonable range, indicating that the structural equilibrium of the complexes within the system was preserved throughout the simulation (Zhao et al., 2023). The RMSD of the four complexes with the lowest binding energy, which ranged from 2 Å to 4 Å over the 0–100 ns interval, are shown in Fig. 4a. RoG and SASA can serve as characterization parameters for assessing changes in protein structure during molecular dynamic simulations. The RoG can also help assess for the assessment of molecular stability and motion characteristics (Zhao et al., 2024). The SASA method enables the prediction of conformational changes upon binding and is widely used for assessing protein accessibility (Pan et al., 2021). The RoG value of the four complexes showed a consistent fluctuation within the range of 21–22 Å throughout the simulation (Fig. 3b-c), demonstrating no significant difference. Additionally, the SASA value of four complexes fluctuated between 16,000–18,000 Å². This observation suggested that the binding of complexes induced minimal conformational changes, thereby demonstrating their remarkable stability. In molecular dynamics simulations of this dynamic system, hydrogen bonds were considered stable when the fluctuation in the number of hydrogen bonds formed between ligands and acceptors is minimal (Zhao et al., 2024). During the 100 ns simulation, a certain number of hydrogen bonds were observed in complexes at any given time (Fig. 3d). These findings demonstrated that the core aroma compounds in coffee husk tea exhibited showed their distinct flavor characteristics by binding to the OR1A1 and OR5M3 receptors.

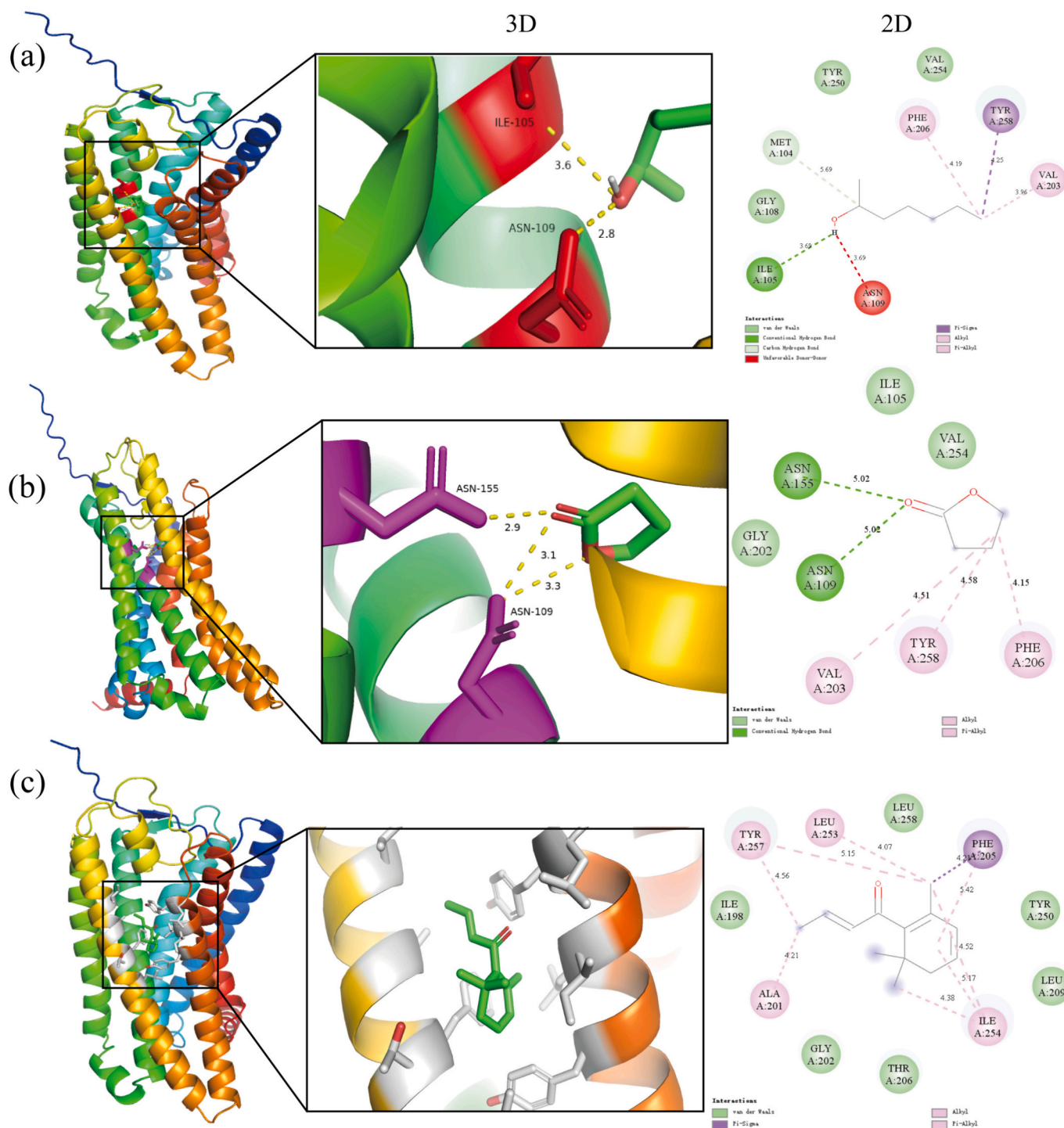


Fig. 2. 3D and 2D molecular docking diagrams depicting the interaction of 4 core volatiles with olfactory receptors. (a) OR1A1–2-heptanol complex; (b) OR1A1–butyrolactone complex; (c) OR5M3–damascenone complex.

3.4. Targeted screening of key aroma compounds

Volatile compounds in food have been noted not only for their aroma characteristics but also for their potential health benefits, including anti-inflammatory and antioxidant properties, as well as their role in regulating insomnia and other chronic diseases (Ayseli & İpek, 2016; Gu et al., 2020; Manyi-Loh et al., 2011). Therefore, the antioxidant and anti-inflammatory effects of 14 key volatile compounds in arabica coffee husk tea were investigated using network pharmacology. A total of 393 targets were identified for these 14 compounds, with benzyl alcohol and

naphthalene showing the highest degree of interaction at 304 (Supplementary Data and Fig. 4a). The network of targets and compounds is shown in Fig. S4. These volatile compounds, commonly found in berries and characterized by high vapor pressure and low boiling point, are typically present in concentrations ranging from parts per billion to parts per million. Furthermore, they not only play a crucial role in sensory perception but also contribute to various health benefits (Gu et al., 2020). Safranal, is a monoterpenoid aldehyde with a sweet aroma, has demonstrated excellent antioxidant and anti-inflammatory activities by decreasing reduced glutathione (GSH) levels and the activities of

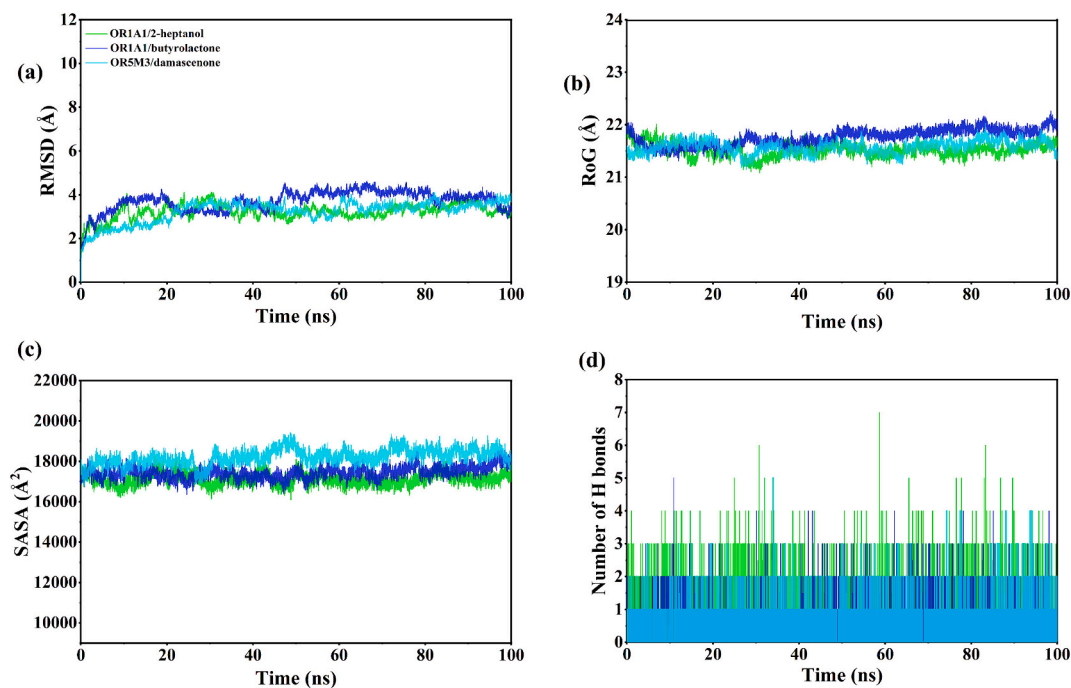


Fig. 3. Molecular simulation analysis of 3 key aroma compounds. (a) The variation of complexes root mean square deviation (RMSD) with time; (b) The change of complexes radius of gyration (RoG) with time; (c) The change of solvent accessible surface area (SASA) with time; (d) Changes in the number of hydrogen bonds between ligands and receptors with time.

superoxide dismutase (SOD) and glutathione-S-transferase (GST), while also increasing the ratio of interferon- γ (IFN- γ) to interleukin-4 (IL-4) in peripheral blood mononuclear cells (Nanda & Madan, 2021). The key volatile benzene derivatives identified in coffee husk tea (Table 1), including benzyl alcohol, 1-methylnaphthalene, and naphthalene, contribute significantly to various biomedical activities such as antiviral, antibacterial, antifungal, antitumor, antioxidant, anti-inflammatory, and immunomodulatory effects (Manyi-Loh et al., 2011).

The targets of these compounds were further analyzed using a Venn diagram to identify key genes associated with antioxidant and anti-inflammatory activities, resulting in the selection of 140 target genes (Fig. 4b), with detailed gene information shown in the Supplementary Data. A PPI network was constructed with high confidence using the STRING database, showing a PPI enrichment p -value of $<1.0 \times 10^{-16}$ (Fig. S5). The visualized PPI network comprised 129 nodes and 1154 edges, with an average node degree of 8.946. Nodes were represented by larger size and darker color to indicate their relative importance. Using the degree as a screening criterion, the top three target genes identified in the antioxidant and anti-inflammatory process were SRC, HSP90AA1, and TNF (Fig. 4c). These genes demonstrated distinct separation from other genes in the scatter plot, further validating their significance (Fig. 4d). SRC family kinases, functioning as nonreceptor tyrosine kinases, are crucial in regulating cell differentiation, proliferation, survival, adhesion, morphology, and motility. Additionally, they play a role in activating the inflammasome (Sekiguchi et al., 2023). Hsp90AA1, a member of the Hsp90 family, plays a crucial role in various pathological and physiological conditions, including cancer, viral infections, oxidative stress, inflammation, and autoimmune diseases (Radhakrishnan et al., 2023). Inhibition of Hsp90 with different pharmacological inhibitors could effectively alleviate a range of inflammatory responses, including macrophage-mediated pro-inflammatory responses, interleukin-1 receptor-associated kinases, TNF, mitogen-activated protein kinase, and SRC-family kinase activation (Rice et al., 2008). Moreover, the TNF family represents a well-established group of factors closely associated with inflammation and oxidative stress (Li et al., 2023 (Li, Wei, et al., 2023; Li, Wu, et al., 2023; Li, Yuan, et al., 2023; Li, Zhou,

et al., 2023)). Hence, the obtained results confirmed that the selected target genes of volatile compounds serve as core candidates for regulating oxidative stress and inflammation.

3.5. GO and KEGG analysis of core target genes

The 140 core target genes were further investigated for key pathways through GO and KEGG enrichment analysis using the DAVID database. The findings revealed 667, 85, and 167 entries associated with biological processes (BP), cellular components (CC), and molecular functions (MF), respectively. Fig. 4e illustrates the top 10 entries. For example, the BP primarily encompassed the cellular response to xenobiotic stimuli, positive regulation of apoptotic processes, and responses to lipopolysaccharides. Notable CC entries comprised membrane rafts, plasma membranes, perinuclear regions of cytoplasm, and related entities. In terms of MF, enriched terms primarily involved enzyme binding, RNA polymerase II transcription factor activity, and ligand-activated sequence-specific DNA binding. Previous studies have demonstrated that naturally derived compounds can alleviate oxidative stress and inflammatory responses induced by H_2O_2 and lipopolysaccharide by modulating relevant enzyme activity (Cao et al., 2023; Yang et al., 2021). These findings effectively demonstrated the potential of volatile compounds in coffee husk tea to mitigate oxidative stress damage and inflammation by influencing various cellular compartments and functions.

Additionally, a total of 135 KEGG signaling pathways associated with oxidative damage and inflammation were identified, with the top 10 pathways illustrated in Fig. 4f. Notably, the targets associated with oxidative damage and inflammation mainly participated in chemical carcinogenesis, lipid and atherosclerosis, and the TNF signaling pathway. The activation of these pathways has been widely documented to trigger oxidative stress and prompt inflammatory responses (Cao et al., 2023). Interestingly, the targeted screening revealed significant identification of TNF proteins within the TNF signaling pathway (Fig. 4c-d). Therefore, the findings of this study suggested that volatile compounds in coffee husk tea exert their antioxidant and anti-

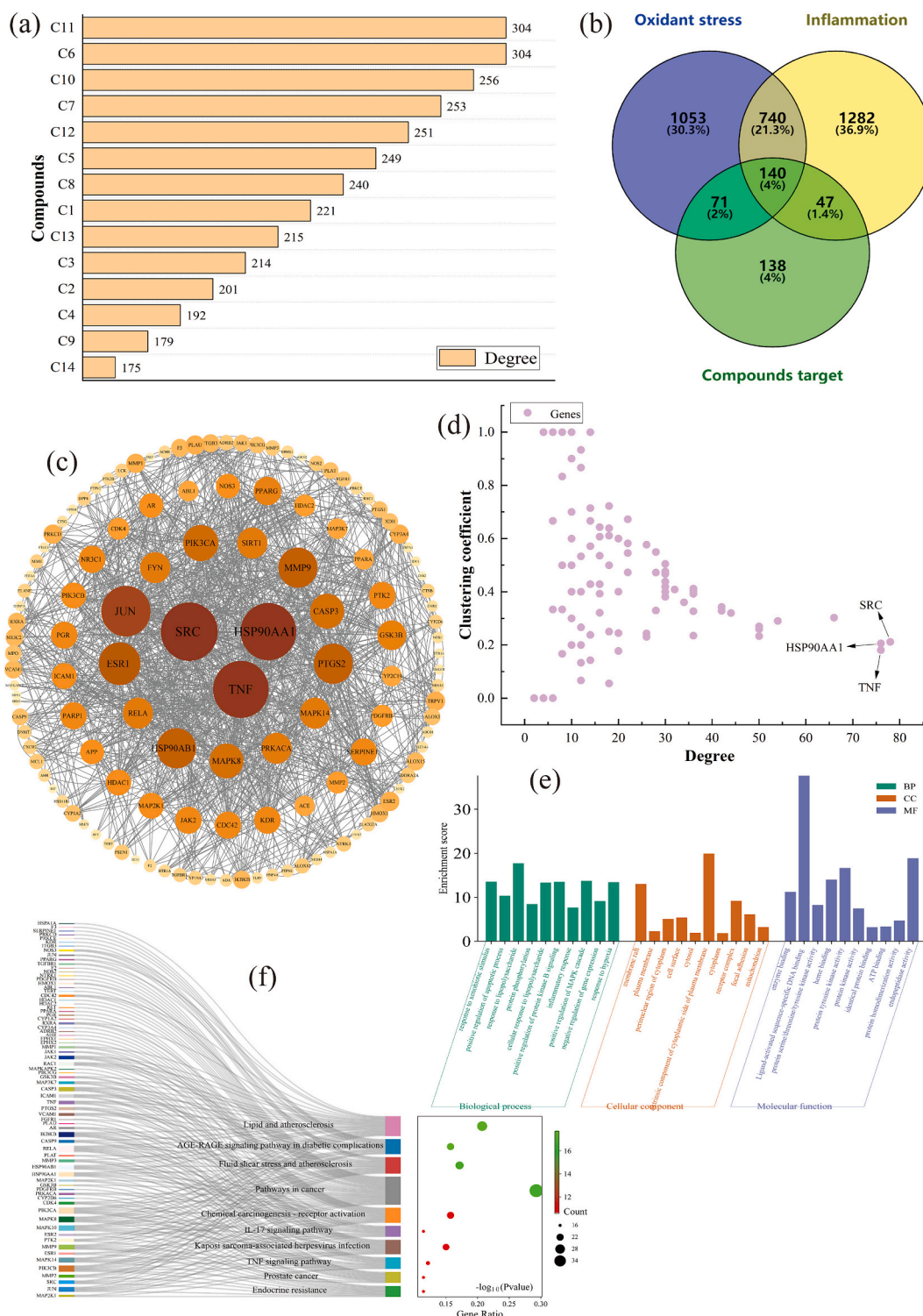


Fig. 4. Targeted screening of 14 different compounds. (a) Volatile compounds degree of coffee husk tea; (b) Venn diagram analysis of target genes; (c) core genes PPI network; (d) the scatter plot of core genes degree; (e) GO analysis of core genes; (f) KEGG enrichment analysis of core genes. C1-C14 represents hexanal, octanal, furfural, 2-heptanol, 2,3-butanediol, benzyl alcohol, 6-methyl-5-hepten-2-one, butyrolactone, damascenone, 1-methylnaphthalene, naphthalene, 1H-pyrazole, 4,5-dihydro-5,5-dimethyl-4-isopropylidene-, 2,2,4,6,6-pentamethylheptane, 1-octadecanesulphonyl chloride.

inflammatory effects by modulating pathways associated with chemical carcinogenesis, lipid metabolism, atherosclerosis, and TNF signaling, among others.

3.6. Molecular simulation verification between volatile compound and targets

In molecular interactions, ligand-receptor binding typically involves a combination of hydrogen bonds, van der Waals interactions, electrostatic interactions, and alkyl interactions. However, hydrogen bonding

is widely recognized as the primary force in this interaction (Asgharzadeh et al., 2024). Table S3 presents the binding affinity of the top 3 screened their respective targets with benzyl alcohol. The results showed that benzyl alcohol binds to the HSP90AA1, TNF, and SRC receptors with the binding energy of -4.7 , -5.2 , and -4.5 kcal/mol, respectively. Furthermore, the targets-benzyl alcohol complexes are primarily stabilized by van der Waals, Pi-sigma, Pi-alkyl, and Pi-cation interactions and hydrogen bonds (Fig. 5). A previous study has reported the significance of van der Waals forces and Pi bonding interactions in facilitating strong binding between ligands and receptors (Zheng et al., 2023). Among the three complexes, the most interaction is van der Waals interaction, followed by hydrogen bond interaction (Fig. 5a-c). In particular, TNF-benzyl alcohol complex only demonstrates van der Waals interactions and hydrogen bond interactions (Fig. 5b).

The stability of these three complexes was further investigated through molecular dynamics simulations to validate their binding affinities. As shown in Fig. 6a, both the HSP90AA1-benzyl alcohol and TNF-benzyl alcohol complexes exhibited lower RMSD values (0.15–0.30 Å) compared to the SRC-benzyl alcohol complex (1–0.45 Å). Notably, the TNF-benzyl alcohol complex exhibited the largest RoG (21.5 Å) and SASA (180–200 Å), suggesting a higher binding potential and stability

between the TNF target and benzyl alcohol within 0–100 ns timeframe (Fig. 6b-c). Throughout the 100 ns simulation, the number of hydrogen bonds was observed in the three complexes range from 0 to 7 (Fig. 6d), indicating the crucial role played by hydrogen bonding during benzyl alcohol binding to the targets. The increase in SASA, hydrogen bonding, and RoG indicated enhanced exposure of the amino acid residues to the aqueous environment, thereby facilitating interaction with surrounding solvent molecules (Asgharzadeh et al., 2024). In addition, the RMSD, RoG, SASA, and hydrogen bonds of the three complexes were basically stable during the 100 ns simulation, indicating that the ligands-receptors binding was stable. Therefore, these results suggested that the key volatile compounds have the potential to bind to core targets and alleviate oxidative stress and inflammation.

4. Conclusion

The present study comprehensively analyzed the key volatile compounds in arabica coffee husk tea, explored their olfactory properties, and assessed their potential antioxidant and anti-inflammatory effects. Sensory evaluation outcomes indicated differences between samples from the C and FC groups. A total of 14 volatile compounds were

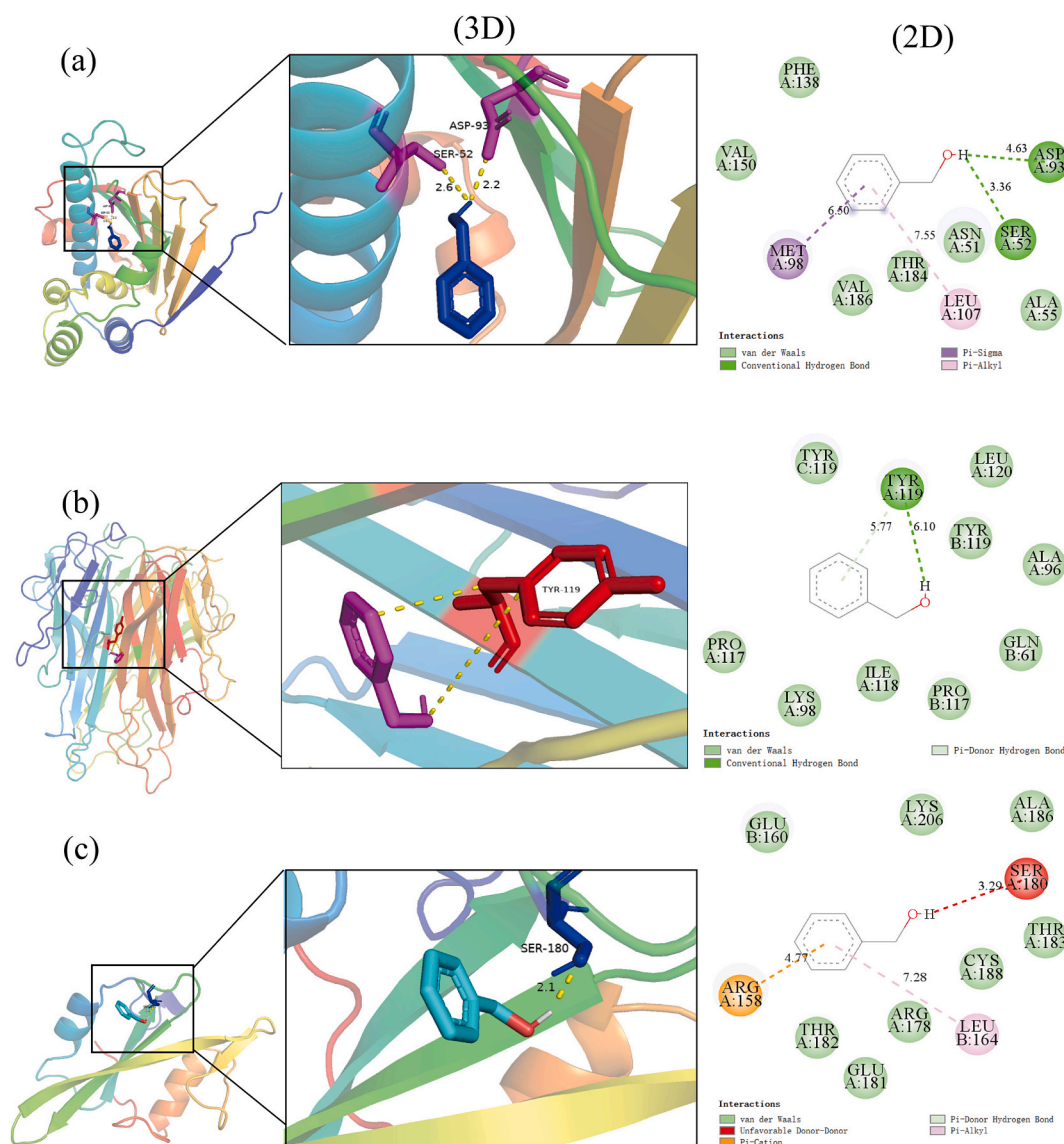


Fig. 5. 3D and 2D molecular docking diagrams of core targets with benzyl alcohol. (a) HSP90AA1-benzyl alcohol complex; (b) TNF-benzyl alcohol complex; (c) SRC-benzyl alcohol complex.

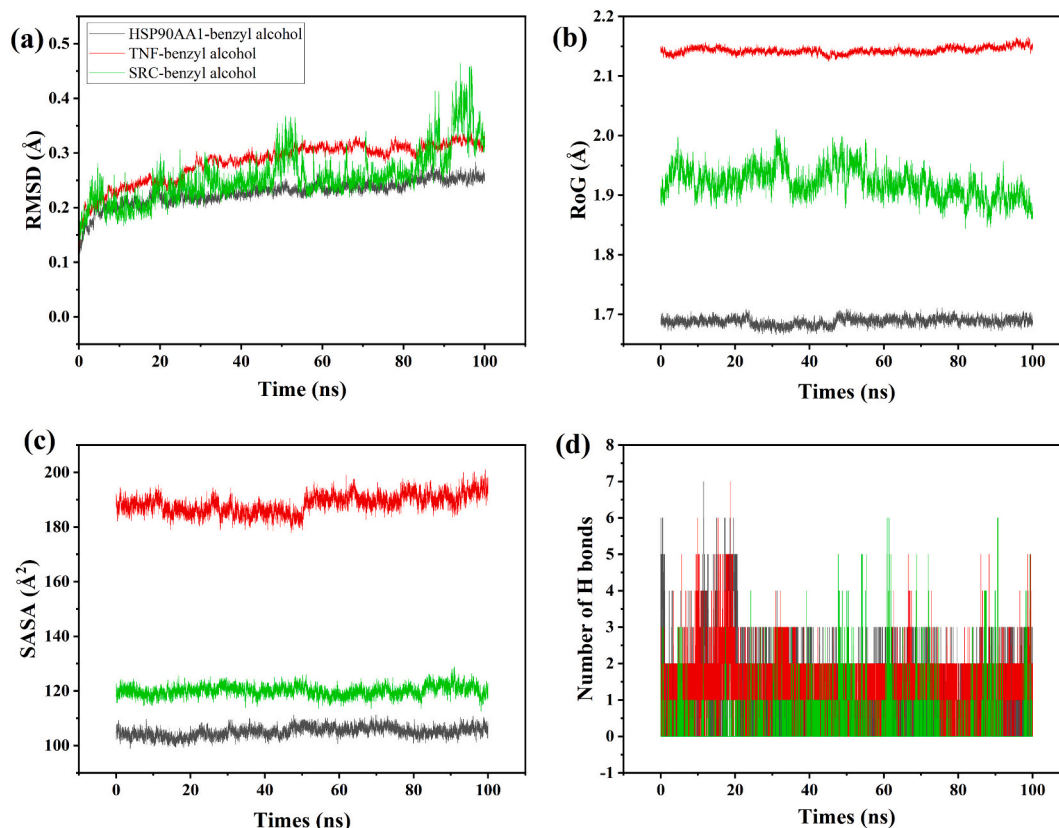


Fig. 6. Molecular simulation analysis of key complexes. (a) The variation of complexes RMSD with time; (b) The change of complexes RoG with time; (c) The change of SASA with time; (d) Changes in the number of hydrogen bonds between ligands and receptors with time.

identified as the significantly different, including 3 aldehydes, 3 alcohols, 3 ketones, 2 naphthalenes, and 3 others. Among these, 5 key aroma compounds ($ROAV \geq 1$) were identified. Furthermore, three key differential compounds ($ROAV \geq 1$) were successfully modeled to form stable complexes with olfactory receptors through molecular docking. Subsequent molecular dynamics simulations validated the stability of these complexes. Furthermore, our investigation revealed that 140 crucial genes associated with oxidative stress and inflammation could be potentially targeted by the 14 identified volatile compounds. These genes are associated with 919 GO terms and 135 KEGG signaling pathways. Through molecular docking and molecular dynamics simulations, it was established that the volatile components present in coffee husk tea may exhibit antioxidant and anti-inflammatory effects by interacting with core receptors through van der Waals, Pi-sigma, Pi-alkyl, and Pi-cation interaction forces. However, it is essential to note that these findings are based solely on computational predictions and require further validation through *in vivo* and *in vitro* experiments.

CRediT authorship contribution statement

Chunyan Zhao: Writing – original draft, Methodology, Formal analysis, Data curation. **Xiuwei Liu:** Writing – review & editing, Validation, Investigation. **Hao Tian:** Supervision, Resources, Project administration, Conceptualization. **Zelin Li:** Writing – review & editing, Writing – original draft, Methodology, Funding acquisition.

Declaration of competing interest

The authors declare that they have no known competing financial interests or personal relationships that could have appeared to influence the work reported in this paper.

Data availability

Data will be made available on request.

Acknowledgements

This research was supported by Introduction and Development of Talents Program of Yunnan Academy of Agricultural Sciences (2024RCYP-14).

Appendix A. Supplementary data

Supplementary data to this article can be found online at <https://doi.org/10.1016/j.fochx.2024.101556>.

References

- Asgharzadeh, S., Shareghi, B., & Farhadian, S. (2024). Structural alterations and inhibition of lysozyme activity upon binding interaction with rotenone: Insights from spectroscopic investigations and molecular dynamics simulation. *International Journal of Biological Macromolecules*, 254, Article 127831. <https://doi.org/10.1016/j.ijbiomac.2023.127831>
- Ayseli, M. T., & İpek, A. Y. (2016). Flavors of the future: Health benefits of flavor precursors and volatile compounds in plant foods. *Trends in Food Science & Technology*, 48, 69–77. <https://doi.org/10.1016/j.tifs.2015.11.005>
- Batista Da Mota, M. C., Batista, N. N., Dias, D. R., & Schwan, R. F. (2022). Impact of microbial self-induced anaerobiosis fermentation (SIAF) on coffee quality. *Food Bioscience*, 47, Article 101640. <https://doi.org/10.1016/j.fbio.2022.101640>
- Cai, X., Wang, S., Wang, H., Liu, S., Liu, G., Chen, H., Kang, J., & Wang, H. (2023). Naringenin inhibits lipid accumulation by activating the AMPK pathway *in vivo* and *in vitro*. *Food Science and Human Wellness*, 12, 1174–1183. <https://doi.org/10.1016/j.fshw.2022.10.043>
- Cao, X., Shi, K., Xu, Y., Zhang, P., Zhang, H., & Pan, S. (2023). Integrated metabolomics and network pharmacology to reveal antioxidant mechanisms and potential pharmacological ingredients of citrus herbs. *Food Research International*, 174, Article 113514. <https://doi.org/10.1016/j.foodres.2023.113514>

- DePaula, J., Cunha, S. C., Cruz, A., Sales, A. L., Revi, I., Fernandes, J., ... Farah, A. (2022). Volatile fingerprinting and sensory profiles of coffee cascara teas produced in Latin American countries. *Foods*, 11(19), 3144. <https://doi.org/10.3390/foods11193144>
- Fang, X., Xu, W., Jiang, G., Sui, M., Xiao, J., Ning, Y., Niaz, R., Wu, D., Feng, X., Chen, J., Huang, Y., & Lei, G. (2024). Monitoring the dynamic changes in aroma during the whole processing of Qingzhuan tea at an industrial scale: From fresh leaves to finished tea. *Food Chemistry*, 439, Article 137810. <https://doi.org/10.1016/j.foodchem.2023.137810>
- Fernandes, A. S., Mello, F. V. C., Thode, F. S., Carpes, R. M., Honório, J. G., Marques, M. R. C., ... Ferraz, E. R. A. (2017). Impacts of discarded coffee waste on human and environmental health. *Ecotoxicology and Environmental Safety*, 141, 30–36. <https://doi.org/10.1016/j.ecoenv.2017.03.011>
- Gao, L., Zhang, L., Liu, J., Zhang, X., & Lu, Y. (2023). Analysis of the volatile flavor compounds of pomegranate seeds at different processing temperatures by GC-IMS. *Molecules*, 28(6), 2717. <https://doi.org/10.3390/molecules28062717>
- Giri, A., Osako, K., & Ohshima, T. (2010). Identification and characterisation of headspace volatiles of fish miso, a Japanese fish meat based fermented paste, with special emphasis on effect of fish species and meat washing. *Food Chem*, 120(2), 621–631. <https://doi.org/10.1016/j.foodchem.2009.10.036>
- Gu, I., Brownmiller, C., Stebbins, N. B., Mauromoustakos, A., Howard, L., & Lee, S. (2020). Berry phenolic and volatile extracts inhibit pro-inflammatory cytokine secretion in LPS-stimulated RAW264.7 cells through suppression of NF-κB signaling pathway. *Antioxidants*, 9(9), 871. <https://doi.org/10.3390/antiox9090871>
- Harini, K., & Sowdhamini, R. (2015). Computational approaches for decoding select odorant-olfactory receptor interactions using mini-virtual screening. *PLoS One*, 10(7), Article e131077. <https://doi.org/10.1371/journal.pone.0131077>
- Heeger, A., Kosińska-Cagnazzo, A., Cantergiani, E., & Andlauer, W. (2017). Bioactives of coffee cherry pulp and its utilisation for production of cascara beverage. *Food Chemistry*, 221, 969–975. <https://doi.org/10.1016/j.foodchem.2016.11.067>
- Hong, Z., Xie, J., Hu, H., Bai, Y., Hu, X., Li, T., Chen, J., Sheng, J., & Tian, Y. (2023). Hypoglycemic effect of *Moringa oleifera* leaf extract and its mechanism prediction based on network pharmacology. *Journal of Future Foods*, 3(4), 383–391. <https://doi.org/10.1016/j.jfutfo.2023.03.009>
- Hou, T., Wang, Y., Dan, W., Wei, Y., Liu, B., Que, T., ... Li, L. (2023). beta-ionone represses renal cell carcinoma progression through activating LKB1/AMPK-triggered autophagy. *Journal of Biochemical and Molecular Toxicology*, 37(6), Article e23331. <https://doi.org/10.1002/jbt.23331>
- Huang, Y., Sun, Y., Mehmood, A., Lu, T., & Chen, X. (2024). Unraveling the temporal changes of Maillard reaction products and aroma profile in coffee leaves during hot-air drying. *Journal of Food Composition and Analysis*, 128, Article 106055. <https://doi.org/10.1016/j.jfca.2024.106055>
- Kristanti, D., Setiaboma, W., Rattawati, L., & Sagita, D. (2022). Robusta coffee cherry fermentation: Physicochemical and sensory evaluation of fermented cascara tea. *Journal of Food Processing and Preservation*, 46(11), Article e17054. <https://doi.org/10.1111/jfpp.17054>
- Lan, Y., Guo, J., Qian, X., Zhu, B., Shi, Y., Wu, G., & Duan, C. (2021). Characterization of key odor-active compounds in sweet petit Manseng (*Vitis vinifera* L.) wine by gas chromatography-olfactometry, aroma reconstitution, and omission tests. *Journal of Food Science*, 86(4), 1258–1272. <https://doi.org/10.1111/1750-3841.15670>
- Li, L., Wei, X., Yang, Z., Zhu, R., Li, D., Shang, G., Wang, H., Meng, S., Wang, Y., Liu, S., & Wu, L. (2023). Alleviative effect of poly-β-hydroxybutyrate on lipopolysaccharide-induced oxidative stress, inflammation and cell apoptosis in *Cyprinus carpio*. *International Journal of Biological Macromolecules*, 253, Article 126784. <https://doi.org/10.1016/j.ijbiomac.2023.126784>
- Li, Q., Li, B., Zhang, C., Zhou, X., Liu, W., Mi, Y., Xie, Z., Li, Y., & Li, J. (2024). Insights into key aroma of vine tea (*Ampelopsis grossedentata*) for grade evaluation integrating relative odor activity value, gas chromatography-olfactometry and chemometrics approaches. *Food Control*, 155, Article 110048. <https://doi.org/10.1016/j.foodcont.2023.110048>
- Li, Y., Wu, T., Deng, X., Tian, D., Ma, C., Wang, X., Li, Y., & Zhou, H. (2023). Characteristic aroma compounds in naturally withered and combined withered γ-aminobutyric acid white tea revealed by HS-SPME-GC-MS and relative odor activity value. *LWT- Food Science and Technology*, 176, Article 114467. <https://doi.org/10.1016/j.lwt.2023.114467>
- Li, Y., Yuan, L., Liu, H., Liu, H., Zhou, Y., Li, M., & Gao, R. (2023). Analysis of the changes of volatile flavor compounds in a traditional Chinese shrimp paste during fermentation based on electronic nose, SPME-GC-MS and HS-GC-IMS. *Food Science and Human Wellness*, 12, 173–182. <https://doi.org/10.1016/j.fshw.2022.07.035>
- Li, Z., Zhou, B., Zheng, T., Zhao, C., Gao, Y., Wu, W., Fan, Y., Wang, X., Qiu, M., & Fan, J. (2023). Structural characteristics, rheological properties, and antioxidant and anti-glycosylation activities of pectin polysaccharides from arabica coffee husks. *Foods*, 12(2). <https://doi.org/10.3390/foods12020423>
- Liang, D., Hu, C., Choupani Chaydarreh, K., Liu, X., Ye, Y., Wei, Y., ... Lin, X. (2022). Volatile components analysis of *Camellia oleifera* shells and related products based on HS-SPME-GC-MS. *Microchem J*, 181, 107842. <https://doi.org/10.1016/j.microc.2022.107842>
- Lin, S., Li, N., Zhou, X., Li, S., Yang, A., Zhou, J., & Liu, P. (2024). Evaluation of perceptual interactions between key aldehydes in kung Pao chicken. *Food Chemistry: X*, 21, Article 101183. <https://doi.org/10.1016/j.fochx.2024.101183>
- Manyi-Loh, C. E., Ndip, R. N., & Clarke, A. M. (2011). Volatile compounds in honey: A review on their involvement in aroma, botanical origin determination and potential biomedical activities. *International Journal of Molecular Sciences*, 12(12), 9514–9532. <https://doi.org/10.3390/ijms12129514>
- Mei, S., & Chen, X. (2023). Combination of HPLC-orbitrap-MS/MS and network pharmacology to identify the anti-inflammatory phytochemicals in the coffee leaf extracts. *Food Frontiers*, 4(3), 1395–1412. <https://doi.org/10.1002/fft2.248>
- Mei, S., Ding, J., & Chen, X. (2023). Identification of differential volatile and non-volatile compounds in coffee leaves prepared from different tea processing steps using HS-SPME/GC-MS and HPLC-Orbitrap-MS/MS and investigation of the binding mechanism of key phytochemicals with olfactory and taste receptors using molecular docking. *Food Research International*, 168, Article 112760. <https://doi.org/10.1016/j.foodres.2023.112760>
- Nanda, S., & Madan, K. (2021). The role of Safranal and saffron stigma extracts in oxidative stress, diseases and photoaging: A systematic review. *Heliyon*, 7(2), Article e6117. <https://doi.org/10.1016/j.heliyon.2021.e06117>
- Pan, F., Li, J., Zhao, L., Tuersuntuoheti, T., Mehmood, A., Zhou, N., Hao, S., Wang, C., Guo, Y., & Lin, W. (2021). A molecular docking and molecular dynamics simulation study on the interaction between cyanidin-3-O-glucoside and major proteins in cow's milk. *Journal of Food Biochemistry*, 45(1), Article e13570. <https://doi.org/10.1111/jfbc.13570>
- Paterson, R. R. M., Lima, N., & Taniwaki, M. H. (2014). Coffee, mycotoxins and climate change. *Food Research International*, 61, 1–15. <https://doi.org/10.1016/j.foodres.2014.03.037>
- Paulino, B. N., Silva, G. N. S., Araújo, F. F., Eri-Numa, I. A. N., Pastore, G. M., Bicas, J. L., & Molina, G. (2022). Beyond natural aromas: The bioactive and technological potential of monoterpenes. *Trends in Food Science & Technology*, 128, 188–201. <https://doi.org/10.1016/j.tifs.2022.08.006>
- Radhakrishnan, A., Mukherjee, T., Mahish, C., Kumar, P. S., Goswami, C., & Chattopadhyay, S. (2023). TRPA1 activation and Hsp90 inhibition synergistically downregulate macrophage activation and inflammatory responses in vitro. *BMC Immunology*, 24(1), 16. <https://doi.org/10.1186/s12865-023-00549-0>
- Rice, J. W., Veal, J. M., Fadden, R. P., Barabasz, A. F., Partridge, J. M., Barta, T. E., ... Hall, S. E. (2008). Small molecule inhibitors of Hsp90 potentially affect inflammatory disease pathways and exhibit activity in models of rheumatoid arthritis. *Arthritis & Rheumatism*, 58(12), 3765–3775. <https://doi.org/10.1002/art.24047>
- Sales, A. L., Cunha, S. C., Morgado, J., Cruz, A., Santos, T. F., Ferreira, I. M. P. L., ... Farah, A. (2023). Volatile, microbial, and sensory profiles and consumer acceptance of coffee cascara Kombuchas. *Foods*, 12(14), 2710. <https://doi.org/10.3390/foods12142710>
- Sales, A. L., Iriondo-DeHond, A., DePaula, J., Ribeiro, M., Ferreira, I., Miguel, M., ... Farah, A. (2023). Intracellular antioxidant and anti-inflammatory effects and bioactive profiles of coffee cascara and black tea Kombucha beverages. *Foods*, 12(9), 1905. <https://doi.org/10.3390/foods12091905>
- Salomon-Ferrer, R., Case, D. A., & Walker, R. C. (2013). An overview of the Amber biomolecular simulation package. *Wiley Interdisciplinary Reviews: Computational Molecular Science*, 3(2), 198–210. <https://doi.org/10.1002/wcms.1121>
- Sekiguchi, Y., Takano, S., Noguchi, T., Kagi, T., Komatsu, R., Tan, M., Hirata, Y., & Matsuzawa, A. (2023). The NLRP3 inflammasome works as a sensor for detecting hypoactivity of the mitochondrial Src family kinases. *The Journal of Immunology*, 210(6), 795–806. <https://doi.org/10.1093/jimmunol.2200611>
- Sevindik, O., Guclu, G., Agirman, B., Selli, S., Kadiroglu, P., Bordiga, M., Capanoglu, E., & Kelebek, H. (2022). Impacts of selected lactic acid bacteria strains on the aroma and bioactive compositions of fermented glaburu (*Viburnum opulus*) juices. *Food Chemistry*, 378, Article 132079. <https://doi.org/10.1016/j.foodchem.2022.132079>
- Sun, Z., Lin, Y., Yang, H., Zhao, R., Zhu, J., & Wang, F. (2024). Characterization of honey-like characteristic aroma compounds in Zunyi black tea and their molecular mechanisms of interaction with olfactory receptors using molecular docking. *LWT- Food Science and Technology*, 191, Article 115640. <https://doi.org/10.1016/j.lwt.2023.115640>
- Tian, M., Lin, K., Yang, L., Jiang, B., Zhang, B., Zhu, X., Ren, D., & Yu, H. (2023). Characterization of key aroma compounds in gray sufu fermented using *Leuconostoc mesenteroides* subsp. *Mesenteroides* F24 as a starter culture. *Food Chemistry: X*, 20, Article 100881. <https://doi.org/10.1016/j.fochx.2023.100881>
- Wan, L., Wang, H., Mo, X., Wang, Y., Song, L., Liu, L., & Liang, W. (2024). Applying HS-SPME-GC-MS combined with PTR-TOF-MS to analyze the volatile compounds in coffee husks of *Coffea arabica* with different primary processing treatments in Yunnan. *LWT- Food Science and Technology*, 191, Article 115675. <https://doi.org/10.1016/j.lwt.2023.115675>
- Wang, Y., Wang, X., Hu, G., Zhang, Z., Al-Romaima, A., Bai, X., Li, J., Zhou, L., Li, Z., & Qiu, M. (2023). Comparative studies of fermented coffee fruits post-treatments on chemical and sensory properties of roasted beans in Yunnan, China. *Food Chemistry*, 423, Article 136332. <https://doi.org/10.1016/j.foodchem.2023.136332>
- Xie, J., Wang, L., Deng, Y., Yuan, H., Zhu, J., Jiang, Y., & Yang, Y. (2023). Characterization of the key odorants in floral aroma green tea based on GC-E-nose, GC-IMS, GC-MS and aroma recombination and investigation of the dynamic changes and aroma formation during processing. *Food Chemistry*, 427, Article 136641. <https://doi.org/10.1016/j.foodchem.2023.136641>
- Xie, R., Chen, F., Ma, Y., Hu, W., Zheng, Q., Cao, J., & Wu, Y. (2023). Network pharmacology-based analysis of marine cyanobacteria derived bioactive compounds for application to Alzheimer's disease. *Frontiers in Pharmacology*, 14, 1249632. <https://doi.org/10.3389/fphar.2023.1249632>
- Xu, J., Zhang, Y., Hu, C., Yu, B., Wan, C., Chen, B., Lu, L., Yuan, L., Wu, Z., & Chen, H. (2024). The flavor substances changes in Fuliang green tea during storage monitoring by GC-MS and GC-IMS. *Food Chemistry: X*, 21, Article 101047. <https://doi.org/10.1016/j.fochx.2023.101047>
- Xu, Y., Wang, Y., Li, R., Sun, P., Chen, D., Shen, J., & Feng, T. (2022). Characteristic aroma analysis of finger citron in four different regions based on GC-MS-HS-SPME and ROAV. *Journal of Food Processing and Preservation*, 46(12), Article e17191. <https://doi.org/10.1111/jfpp.17191>

- Yang, Z., Mo, Y., Cheng, F., Zhang, H., Shang, R., Wang, X., Liang, J., Liu, Y., & Hao, B. (2021). Antioxidant effects and potential molecular mechanism of action of *Limonium aureum* extract based on systematic network pharmacology. *Frontiers in Veterinary Science*, 8, Article 775490. <https://doi.org/10.3389/fvets.2021.775490>
- Zhao, S., Ma, S., Zhang, Y., Gao, M., Luo, Z., & Cai, S. (2024). Combining molecular docking and molecular dynamics simulation to discover four novel umami peptides from tuna skeletal myosin with sensory evaluation validation. *Food Chemistry*, 433, Article 137331. <https://doi.org/10.1016/j.foodchem.2023.137331>
- Zhao, W., Zhang, Q., Su, L., & Yu, Z. (2023). Taste characteristics and umami mechanism of novel umami peptides from hen egg proteins. *LWT- Food Science and Technology*, 181, Article 114778. <https://doi.org/10.1016/j.lwt.2023.114778>
- Zheng, X., Chi, H., Ma, S., Zhao, L., & Cai, S. (2023). Identification of novel α -glucosidase inhibitory peptides in rice wine and their antioxidant activities using *in silico* and *in vitro* analyses. *LWT- Food Science and Technology*, 178, Article 114629. <https://doi.org/10.1016/j.lwt.2023.114629>